analytical chemistry

pubs.acs.org/ac Article

Structural Characterization of Isomeric Oligogalacturonan Mixtures Using Ultrahigh-Performance Liquid Chromatography-Charge Transfer Dissociation Mass Spectrometry

Praneeth M. Mendis, Zachary J. Sasiene, David Ropartz, Hélène Rogniaux, and Glen P. Jackson*

Cite This: *Anal. Chem.* 2021, 93, 2838−2847 Read Online

ACCESS | Metrics & More | Article Recommendations | Supporting Information

ABSTRACT: Pectins are natural polysaccharides made from galacturonic acid residues, and they are widely used as an excipient in food and pharmaceutical industries. The degree of methyl-esterification, the monomeric composition, and the linkage pattern are all important factors that influence the physical and chemical properties of pectins, such as the solubility. This work focuses on the successful online coupling of charge transfer dissociation−mass spectrometry (CTD-MS) with ultrahigh-performance liquid chromatography (UHPLC) to differentiate isomers of oligogalacturonans derived from citrus pectins. This work employed CTD fragmentation of the pectin mixtures in data-dependent acquisition mode. Compared to the UHPLC with collision-induced dissociation mass spectrometry (UHPLC-CID-MS), UHPLC-CTD-MS yielded fewer ambiguous ions and more structurally informative results. The developed UHPLC-CTD-MS method resulted in abundant cross-ring cleavages—and especially $^{1,4}X_n$, $^{1,5}X_n$, and $^{2,4}X_n$ ions—which helped to identify most of the isomers. The Gal A isomers differed only in the methyl group position along the galacturonic acid backbone. The combination of CTD in real time with UHPLC provides a new tool for the structural characterization of complex mixtures of oligogalacturonans and potentially other classes of oligosaccharides.

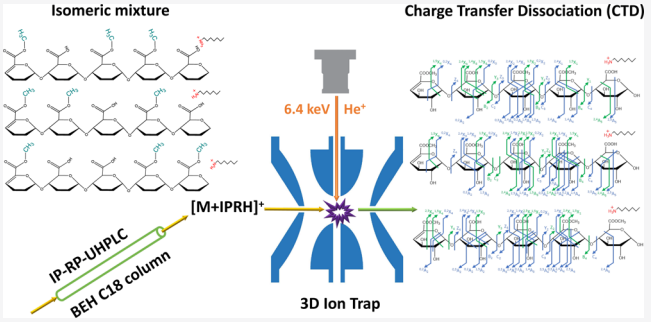

INTRODUCTION

Oligogalacturonans are composed of different degrees of polymerization (DPs) of galacturonic acid (Gal A) residues.[1−4] These Gal A residues can be methyl esterified, acetylated, or both, which results in complex and heterogeneous oligomeric structures.[3] A major natural source of oligogalacturonans are plant-based pectins, which have structural and functional roles in the plant cell wall and middle lamella region.[2] Pectins mainly consist of linear chains of α-1,4-linked Gal A monomers.[3,4] Pectins play a vital role in food, pharmaceutical, textile, and paper industries because of the unique gelling, thickening, and stabilizing properties.[1,2] The physical and chemical properties of pectin are strongly influenced by the degree and pattern of methyl esterification of Gal A residues,[1,4,5] so it is important to develop methods of analysis that can effectively characterize the different structures.

Tandem mass spectrometry (MS/MS) is a common analytical technique used for the structural characterization of polysaccharides, including pectins, because of its sensitivity, short analysis time, low sample consumption, and the high information content.[1,3] Collision-induced dissociation (CID) is the most popular MS/MS technique for oligosaccharide characterization, including methyl-esterified Gal-A residues.[6] However, CID predominantly results in glycosidic bond cleavages such as B/Y and C/Z fragments, which tend not to provide sufficient detail to elucidate linkage isomers and methyl-esterification positions within the sugar residues.[7] Also, the interpretation of CID mass spectra for oligosaccharides is complicated by neutral losses, rearrangements, and internal fragments that are derived from two different fragmentation sites.[1,8−10]

Alternative methods to CID, such as ion/electron interactions, are also used in the structural characterization of oligosaccharides. Electron transfer dissociation (ETD)[11] and electron capture dissociation (ECD)[12] have been applied to multiply charged positive oligosaccharides,[13] whereas negative ETD,[14,19,20] electron detachment dissociation (EDD),[15,16,21] electron excitation dissociation (EED),[17] and electron-induced dissociation (EID)[18] have been applied to the analysis of oligosaccharides in negative mode.[1,7,12,13] ETD and ECD are limited to multiply charged positive ions; therefore, the native analysis of pectins whose methyl-esterification tends to inhibit the generation of high charge states are generally resistant to

Received: October 1, 2020
Accepted: January 12, 2021
Published: January 26, 2021

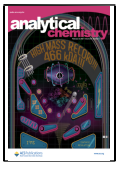

https://dx.doi.org/10.1021/acs.analchem.0c04142
Anal. Chem. 2021, 93, 2838−2847

structural interrogation by ECD and ETD.[1,7,14] EID and EED have the advantage that they are effective for singly charged ions[17,18] but historically have been restricted to the Fourier-transform ion cyclotron resonance mass analyzers, which are cost-prohibitive for most laboratories. However, ECD and EID have recently been implemented on benchtop, hybrid instruments, and the figures of merit are still under assessment.[22]

Photoactivation is another genre of gas-phase activation for glycan characterization, including vacuum ultraviolet photodissociation (VUVPD)[23] and extreme ultraviolet dissociative photoionization (XUV-DPI), both of which have sufficient energy to obviate the need for specific chromophores.[24] VUVPD at 157 nm can generate both glycosidic cleavages (B/Y and C/Z) as well as particularly useful A- and X-type fragments of oligosaccharides,[25,26] but the use of a 157 nm laser requires an additional vacuum coupling to evacuate the beamline and prevent photon absorption in air.[27] XUV-DPI requires a synchrotron radiation source to produce the intense photon beam with a photon energy in excess of 16 eV, which clearly limits the widespread adoption by other laboratories.[8]

Free radical-activated glycan sequencing (FRAGS) of reagents is an alternative method inspired by the free radical-driven dissociation techniques.[28] FRAGS is capable of producing both glycosidic bonds and cross-ring cleavages without generating glycan rearrangements and internal and external residue losses upon collisional dissociation.[28,29] Charge transfer dissociation (CTD) is a novel ion activation method that provides such capabilities, and, despite its own drawbacks, CTD has shown promising results for oligosaccharides, peptides, proteins, and lipids.[8,30−32]

Several groups helped lay the foundation for the development of CTD. For example, Schlathölter's group used kiloelectronvolt hydrogen and helium cations to dissociate leucine encephalin,[33,34] and Zubarev's group used 1−3 keV beams containing a mixture of $O_2^{+\bullet}$ and $N_2^{+\bullet}$ exiting a microwave plasma to analyze multiply charged angiotensin I and ubiquitin precursor ions.[35] Schlathölter's group showed that helium cations in the region of 2−10 keV have the ability to abstract an electron from a singly charged protonated precursor ion and form a doubly charged radical ion via two competing pathways: charge transfer and electron stopping.[33,34]

$$\text{Charge transfer: } [M + H]^+ + He^+ \rightarrow [M + H]^{2+\bullet *} + He \rightarrow \text{fragments} \quad (1)$$

$$\text{Electron stopping: } [M + H]^+ + He^+ \rightarrow [M + H]^{2+\bullet *} + He^+ + e^- \rightarrow \text{fragments} \quad (2)$$

Regardless of the exact mechanism above, ion activation using the kiloelectronvolt reagent ions leads to radical-driven fragmentation.[33,36] Hoffmann and Jackson expanded the previously conducted experiments by installing a rare-gas ion gun to a two-dimensional (2D) ion trap to accomplish He-CTD of a singly charged substance P.[36] Helium cations were chosen because they have the largest electron affinity of all singly charged cations at 24.6 eV. The Jackson group then modified a three-dimensional (3-D) ion trap to accomplish CTD, and the latter instrument has been a useful tool in the analysis of oligosaccharides because it provides extensive fragmentation while generating structurally informative fragments such as A and X ions.[8,30,37] Although CTD is not commercially available, the technique can be implemented with a few modifications on commercially available 2D and 3D ion trap instruments.[25−28]

Recent efforts in the development of analytical methodologies for complex oligosaccharide analysis have coupled chromatographic techniques with MS/MS to enhance structural characterization of complex mixtures,[38−40] including high pH anion exchange chromatography (HPAEC),[41] size exclusion chromatography (SEC),[42] hydrophilic interaction chromatography (HILIC),[42] reversed-phase liquid chromatography (RPLC),[43] and porous graphitized carbon (PGC) chromatography.[44] RPLC-MS/MS and PGC-MS/MS have recently been successfully implemented for the structural characterization of isomeric glycans,[20,38,45,46] but PGC tends to require long conditioning times between runs to provide reproducible separations, which is mildly detrimental to routine analyses.[39,47] Therefore, the work herein uses (RPLC coupled with a volatile ion-pairing agent (IP) because it has successfully been used in oligosaccharide analyses,[1,48] heparin-derived oligosaccharides,[40] chondroitin sulfates,[46] carrageenans,[48] porphyrans[49] and Gal A samples.[1]

The current work demonstrates that CTD-MS spectral acquisition rates are fast enough to enable their coupling with ion-paired reversed-phase ultrahigh-performance liquid chromatography (IP-RP-UHPLC) for the analysis of a complex oligosaccharide mixture derived from citrus fruit pectins. The effectiveness of the obtained results from IP-RP-UHPLC-CTD-MS was compared to results obtained using IP-RP-UHPLC-CID-MS on the same instrument, and the CTD spectra contained more cross-ring fragments and fewer neutral losses, both of which assisted the spectral and structural characterization of the previously characterized Gal A mixture from DP3 to DP6 with degrees of methyl-esterification (DM) from DM1 to DM4.[1] UHPLC-CTD-MS successfully elucidated the structures of several Gal A isomers, which were chromatographically resolved using IP-RP-UHPLC.

EXPERIMENTAL SECTION

Details of the experimental procedure are provided in the Supporting Information.

Briefly, a prepared complex mixture of oligogalacturonans (HGB69) was donated by the French National Research Institute for Agriculture, Food, and the Environment (INRAE) (Nantes, France). The mixture of highly methylated homogalacturonans was enzymatically digested by pectin lyase and was obtained from citrus fruit according to the method described by Ralet et al.[4] The mixture was separated using IP-RP-HPLC on a Shimadzu Nexera X2 UHPLC system (Kyoto, Japan) using a Waters BEH C18 column with the following dimensions: 100 mm × 1.0 mm, packed with 1.7 μm porosity particles (Wexford, Ireland). A binary gradient was ramped from 2.5% methanol to 73% methanol over 27.5 min with a constant concentration of ion pair reagent of 20 mM heptylammonium formate. The effluent from the UHPLC was connected to the standard Bruker Apollo electrospray ionization source (Billerica, MA). CTD was performed on a modified Bruker amaZon ETD 3D ion trap from Bruker Daltonics (Bremen, Germany), as described previously and as given in the Supporting Information.[36] During CTD, the precursor ions were stored at a low mass cutoff (LMCO) of $m/$

https://dx.doi.org/10.1021/acs.analchem.0c04142
Anal. Chem. 2021, 93, 2838−2847

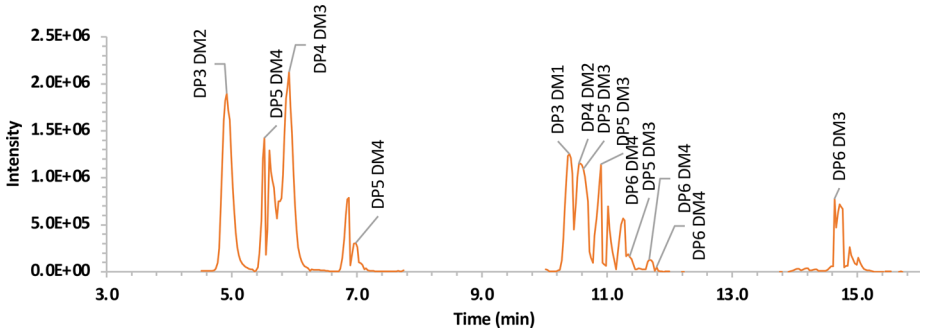

Figure 1. Reconstructed ion chromatogram of molecular ions obtained during data-dependent CTD acquisition. DP = degree of polymerization; DM = degree of methyl esterification.

Table 1. Summary of oligogalacturonans separated using the IP-RP-UHPLC gradient that were exposed to either He-CTD or CID[a]

Oligosaccharide	MW (Da)	Nominal *m/z* $[M+IPRH]^+$	Retention time (min)	# Free carboxylic acid groups	Structure
DP3DM2	556.1	672	4.90	1	
DP5DM4	936.2	1052	5.60	1	
	936.2	1052	7.00	1	
DP5DM3	922.2	1038	10.57	2	
	922.2	1038	10.90	2	
	922.2	1038	11.36	2	
DP6DM4	1112.3	1228	11.25	2	
	1112.3	1228	11.73	2	
	1112.3	1228	11.82	2	
DP6DM3	1098.2	1214	14.64	3	

[a]Full circles represent methyl-esterified Gal As, empty circles represent free Gal As. Red diagonal lines on the non-reducing terminal residues indicate the presence of double bonds, which are derived from the enzymatic hydrolysis with a lyase.

z 300 to minimize the chemical background in the low mass region. The 50 ms pulses of helium cations from the reagent ion gun had a kinetic energy of approximately 6.4 keV, and the CID amplitude was set to zero during CTD to prevent collisional activation. In contrast, during the CID experiments, the ion gun was deactivated, the LMCO was set to 27% of the precursor ion *m/z* value, and ions were fragmented using the "smart fragmentation" feature at 0.7 V for 200 ms.

RESULTS AND DISCUSSION

Figure 1 shows the reconstructed total ion chromatogram of the complex mixture of oligogalacturonans generated by the enzymatic degradation of highly methylated homogalacturonans derived from citrus pectins (HGB69). The total ion chromatogram (TIC) is provided in Figure S1. As has been established previously,[1] the elution order of the oligogalacturonan components correlates most strongly with the number of free carboxylic acid groups in the oligosaccharides, then according to differences in the DP, the degree of methylesterification (DM), and the pattern of methyl esterification.

As shown by the elution times in Table 1, IP-RP-UHPLC can separate isomeric oligosaccharides that differ only in their spatial arrangement of the methyl groups. This table also displays the precursor ion *m/z* values that were isolated and exposed to either CID or He-CTD to enable isomer differentiation. The chromatographic peaks and tandem mass spectra reviewed indicate that there are three major isomeric structures for the DP5DM3 and DP6DM4 compounds and two major isomers for DP5DM4.[1]

Figure 2 shows the CID and He-CTD spectra obtained for the DP6DM3 isomer eluting at 14.64 min. The precursor activated in the spectrum is the $[M + IPRH]^+$ ion at *m/z* 1214.38. CID produced a series of glycosidic and cross-ring cleavages. Major peaks correspond to the fragment types B, Y, Z, $^{2,4}A_n$, $^{0,2}X_n$, and $^{1,5}X_n$. $^{1,5}X_n$ ions are commonly observed in the CID of low charge state oligosaccharides,[50] and although they are a type of cross-ring fragment, they are not any more structurally informative than glycosidic cleavages.[51] Using CID, fragmentation mainly transpired in the middle Gal A units of the oligogalacturonan structure. The observed fragments do not provide sufficient information on the reducing and nonreducing ends. Also, the majority of the observed fragments are accompanied by neutral losses, as indicated by the circles, diamonds, and daggers in the annotations. The lack of retention of the methyl groups introduces uncertainty to structural identification and significantly complicates the spectral interpretation.

In contrast to the CID spectrum in Figure 2a, neutral losses of methanol are less commonly observed in the He-CTD spectrum shown in Figure 2b. The He-CTD spectrum instead contains an abundance of fragments that show the loss of a neutral IPR group (−115 Da) and one or two water molecules. The extensive cross-ring cleavages and the minimum methanol losses in He-CTD were beneficial in determining the positions of methyl-esterification and the branching pattern.

The He-CTD spectrum shown in Figure 2b shows that a systematic series of fragments are produced throughout the structure, including ions identified as $^{0,3}A_n$, $^{1,4}A_n$, $^{1,5}X_n$, $^{1,4}X_n$, and $^{0,2}X_n$. The monomeric sequence can also be explained with the sequence of glycosidic Y cleavages, which is similar to CID results. Fragments such as Y_2, Y_4, and Y_5 were used to identify the methylated Gal A units present toward the reducing end. The Y_5 fragment contains two methyl groups, which help to localize the first methyl esterification site on the first Gal A unit

https://dx.doi.org/10.1021/acs.analchem.0c04142
Anal. Chem. 2021, 93, 2838−2847

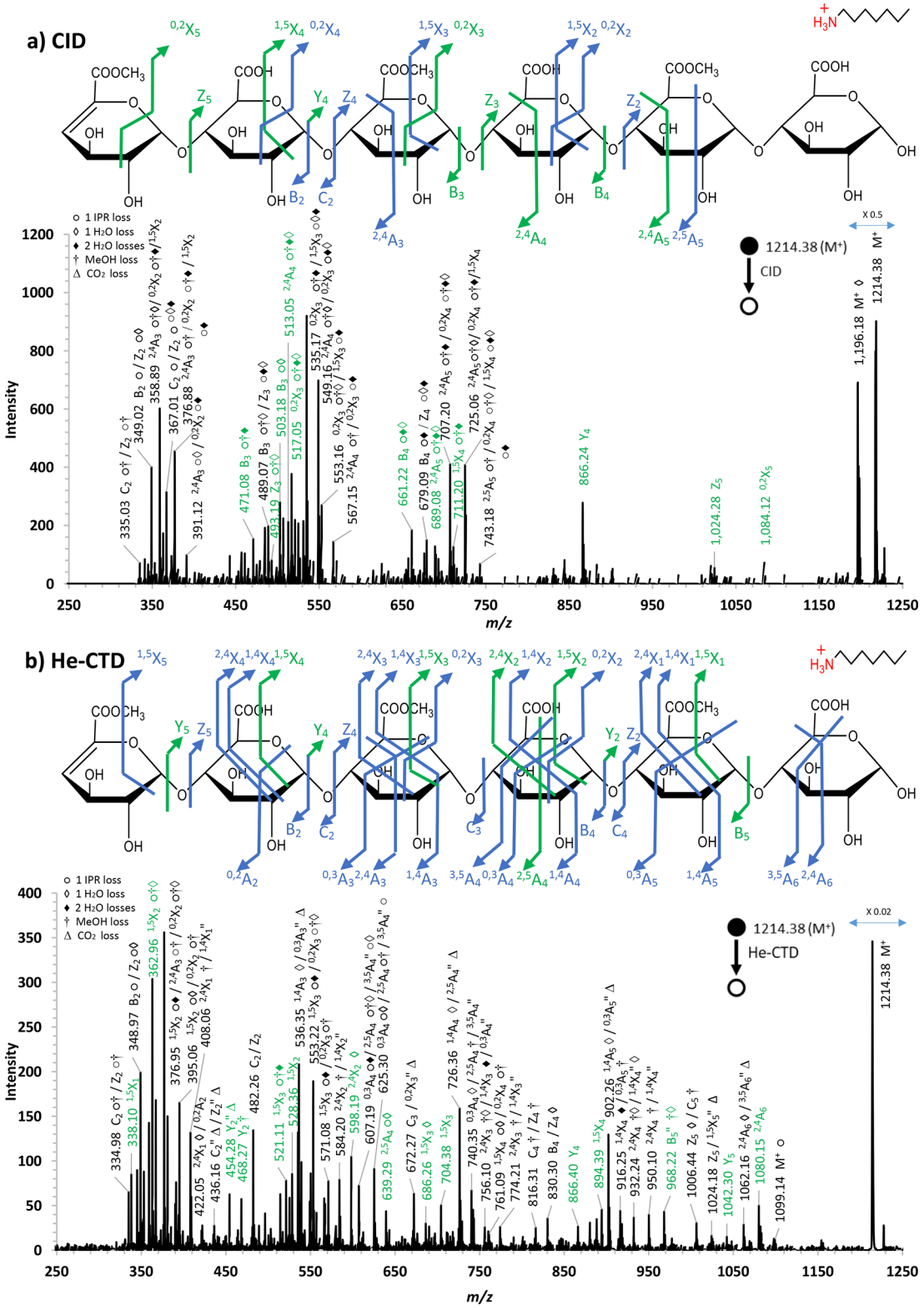

Figure 2. IP-RP-UHPLC-MS spectra of the oligogalacturonan DP6DM3 at 14.64 min collected in positive ion mode via (a) CID and (b) He-CTD. The insets show the annotated product ions. Fragments with unambiguous assignments are annotated in green. The precursor ion was isolated at m/z 1214.38 as $[M + IPRH]^+$ species.

at the nonreducing end. The second methylated Gal A unit can be localized with the aid of the Y_4 and $^{1,5}X_3$ fragment pair. The third methyl group position can be localized with the aid of the Y_2 and $^{1,5}X_1$ fragment pair, which is located on the second Gal A unit from the reducing end. In short, He-CTD was able to unambiguously assign the sugar residues that contain the three methyl groups, but CID could not.

The molecular ions of DP5DM4 (m/z 1052.37) and DP5DM3 (m/z 1038.35) were also selected as test cases because the molecular ions of each oligogalacturonan provided

https://dx.doi.org/10.1021/acs.analchem.0c04142
Anal. Chem. 2021, 93, 2838−2847

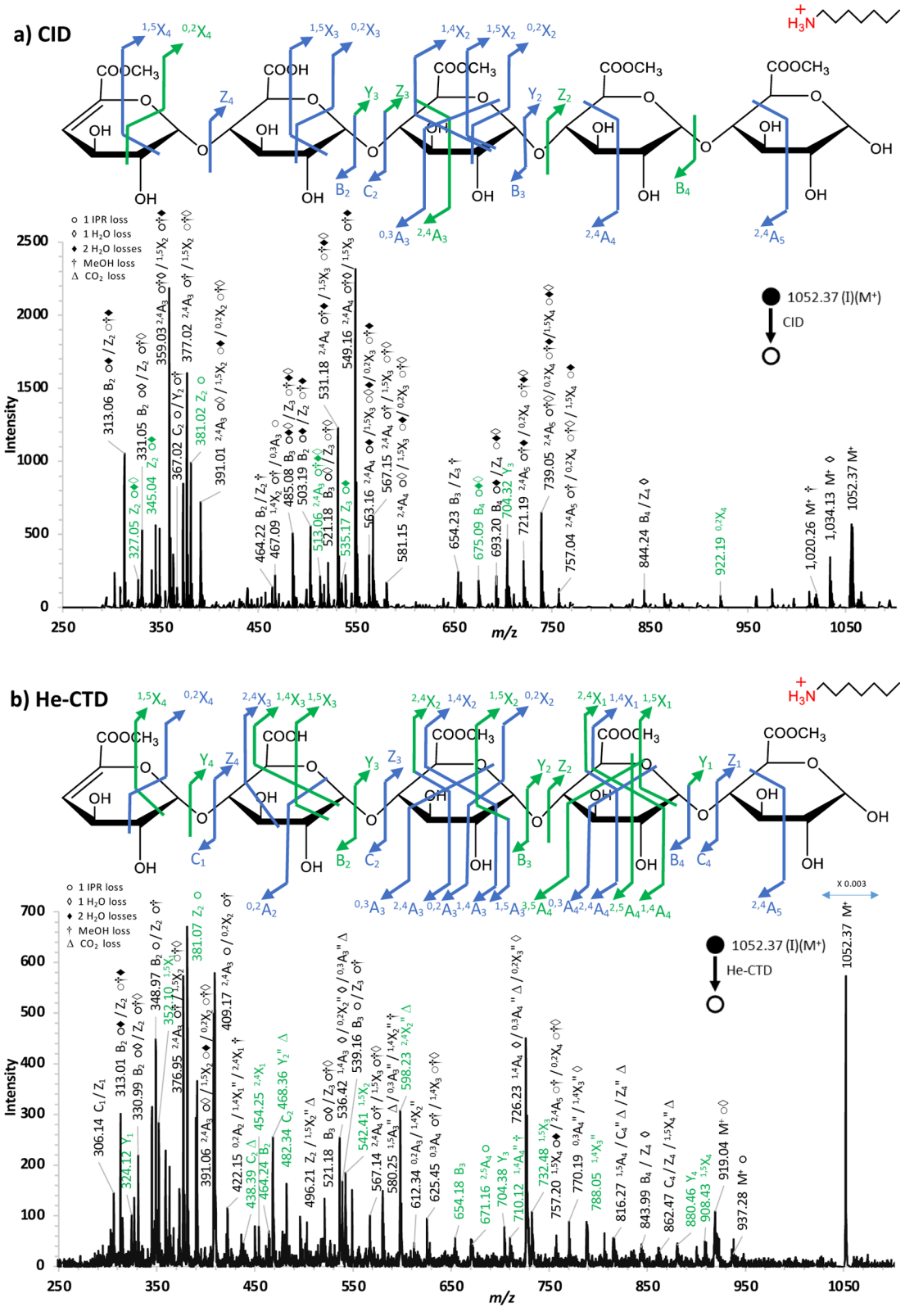

Figure 3. IP-RP-UHPLC-MS/MS spectra of oligogalacturonan DP5DM4 isomer I at 5.6 min collected in positive ion mode using (a) CID and (b) He-CTD. The insets show the annotated product ions. Fragments with unambiguous assignments are annotated in green. The precursor ion was isolated at m/z 1052.37 as $[M + IPRH]^+$ species.

two obvious structural isomers in the reconstructed ion chromatogram. The isomerism arises from differences in the methyl esterification position of each structure. The two isomers of DP5DM4 elute at 5.6 (isomer I) and 7.0 min (isomer II), and the resulting CID and He-CTD spectra for each isomer are shown in Figure 3a and **3b**, respectively. Similar to the DP6DM3 results, CID produces a series of consecutive neutral losses of H_2O, IPR, and MeOH and these

https://dx.doi.org/10.1021/acs.analchem.0c04142
Anal. Chem. 2021, 93, 2838−2847

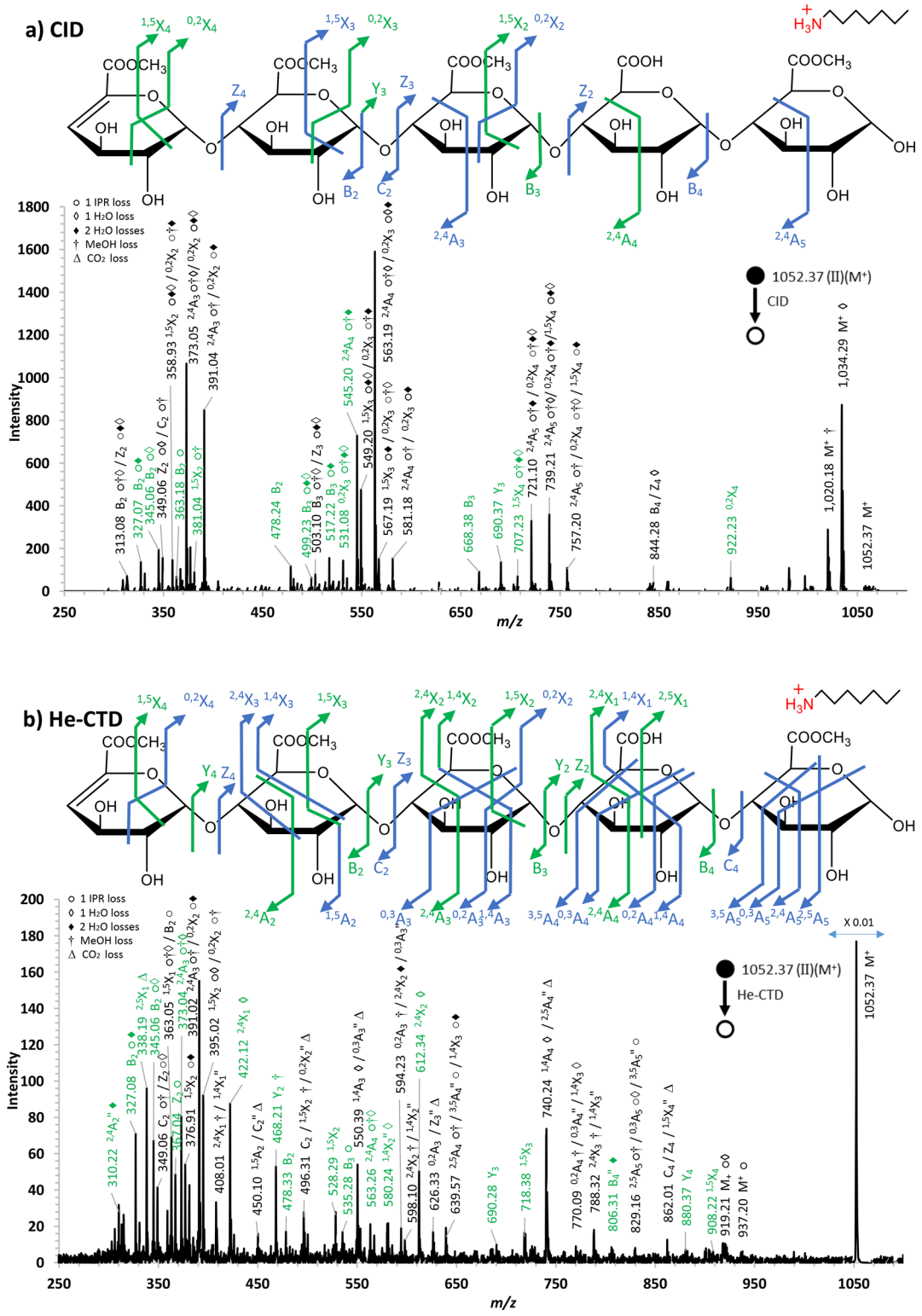

Figure 4. IP-RP-UHPLC-MS/MS spectra of oligogalacturonan DP5DM4 isomer II at 7.0 min collected in positive ion mode using (a) CID and (b) He-CTD. The insets show the annotated product ions. Fragments with unambiguous assignments are annotated in green. The precursor ion was isolated at m/z 1052.37 as $[M + IPRH]^+$ species.

neutral losses complicate the spectral interpretation. In addition to the glycosidic cleavages, CID provides a series of peaks that contain multiple possible identities, each consisting of multiple neutral losses from one or more of $^{2,4}A_n$, $^{1,5}X_n$, or $^{0,2}X_n$ ions. For example, the peak at m/z 739.05 could be one or more of $[^{2,4}A_5 - IPR - MeOH - H_2O]$, $[^{1,5}X_4 - IPR - 3H_2O]$, and $[^{0,2}X_4 - IPR - MeOH - 2H_2O]$. Supporting these assignments are additional peaks shifted by +18 and −18 Da relative to the peaks above, which correspond to one less or one more neutral water loss, respectively.

Isomers I and II can be differentiated using the CID glycosidic cleavages of B_n and Y_n. For example, the Y_3 fragment

https://dx.doi.org/10.1021/acs.analchem.0c04142
Anal. Chem. 2021, 93, 2838−2847

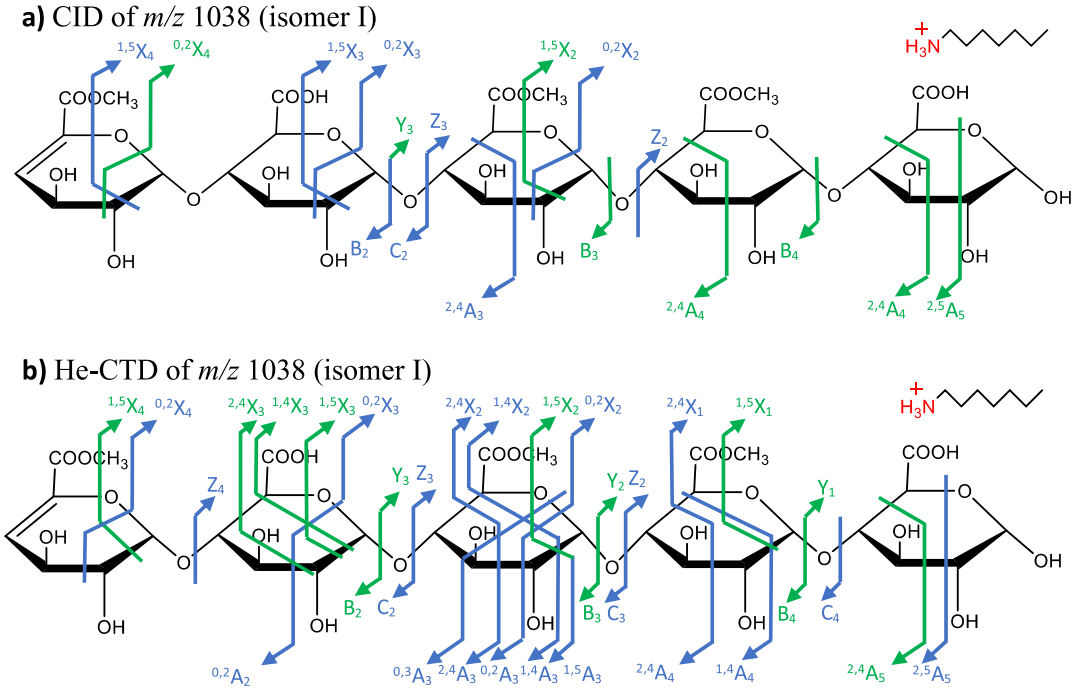

Figure 5. Fragmentation patterns for oligogalacturonan DP5DM3 (isomer I) eluting at 10.6 min. Blue annotations are ambiguous because of alternative isobaric annotations. Green annotations are unambiguous.

from isomer I given in Figure 3a gives the indication that three out of four methylated sites are located within the first three Gal A units at the reducing end. Similarly, the Y_3 fragment of isomer II shown in Figure 4a contains only two methylated sites that are located on the three Gal A units at the reducing end. The B_3 fragment from isomer II confirms the presence of three methylated sites toward the nonreducing end, which distinguishes this isomer from isomer I. The characteristic $^{0,2}X_4$ fragment in the CID spectra of both isomers helps to identify the presence of a methyl-esterification site at the nonreducing end. Even though the results of CID can be used to distinguish the two isomers using glycosidic cleavages, it is difficult to localize the methylated sites within each Gal A unit because of the extensive neutral losses, especially the neutral losses of methanol.

The He-CTD spectra given in Figures 3b and 4b for isomers I and II, respectively, provide fewer neutral losses and richer fragmentation, which include a more dominant contribution of cross-ring cleavages than CID. An advantage with He-CTD is the generation of a series of intact $^{1,5}X_n$ product ions for both isomers, which enable the localization of the three main methylated positions on Gal A units present toward the reducing end. For example, the methyl groups can be easily localized with the pairs $^{1,5}X_3-Y_4$, $^{1,5}X_2-Y_3$, and $^{1,5}X_1-Y_2$. Fortuitously, the m/z values of the $^{1,5}X_n$ ions share no isobars and are therefore unambiguous. Possible fragments observed at the nonreducing end such as $^{1,5}X_4$ and $^{0,2}X_4$ help to localize the fourth methylated site on the Gal A unit at the nonreducing end. Heavy oxygen labeling (^{18}O) was not performed in these experiments but has been used successfully in the past to help differentiate ions originating from the reducing and nonreducing termini.[1,8] The absence of ^{18}O labeling causes a reduction in the confidence during the identification of symmetric fragments, such as C_n and Z_n in an unknown sample because of the presence of the unsaturated bond at the nonreducing end, which can lead to the misassignment of fragments.

In addition to the glycosidic cleavages and characteristic $^{1,5}X_n$ fragments, the unambiguous $^{2,4}X_1$ fragment is present at m/z 454.25 for isomer I and m/z 422.12 for isomer II, as shown in Figures 3b and 4b, respectively, and can be used to distinguish between the two isomers. The $^{2,4}X_1$ fragment indicates the presence of two methyl-esterification sites for isomer I and one methyl-esterification site for isomer II at the two Gal A units at the reducing end. 6-*O*-methylation can be identified with the combination of different A and X fragments. As an example, in isomer II, the Y_2-Y_3 fragment pair proves the presence of a methylated site on the central Gal A unit in DP5DM4. By using the $^{1,5}X_2-^{1,4}X_2$ fragment pair, the methylated site can be narrowed down to the 6-*O* position. Moreover, He-CTD is capable of providing details regarding the linkages among monosaccharide units in oligomers.[52] For example, the $^{1,5}X_2$, $^{2,4}X_1$, and $^{3,5}A_4/^{0,3}A_4$ fragments provide evidence for the presence of a 1−4 linkage among the third and fourth Gal A units in isomer I. Such specific linkage information is not possible with CID results because of the limited number of cross-ring fragments.

Another abundant component in the oligogalacturonan mixture has the molecular assignment DP5DM3, of which there are up to 10 theoretical permutations of structures. In practice, only three constitutional isomer peaks were abundant in the mixture and each was analyzed using CID and He-CTD. In CID, the $^{1,5}X_n$ ions were accompanied by the neutral losses of an ion pair reagent and two water molecules, which is indistinguishable from an $^{0,2}X_n$ ion with the neutral losses of an ion pair reagent and a molecule each of water and methanol. In He-CTD, the $^{1,5}X_n$ ions were observed with one or no neutral losses, so oftentimes they did not have as many isobaric alternatives.

The three isomeric structures of DP5DM3 labeled I−III elute at 10.6, 10.9, and 11.4 min, respectively. The isomeric

https://dx.doi.org/10.1021/acs.analchem.0c04142
Anal. Chem. 2021, 93, 2838−2847

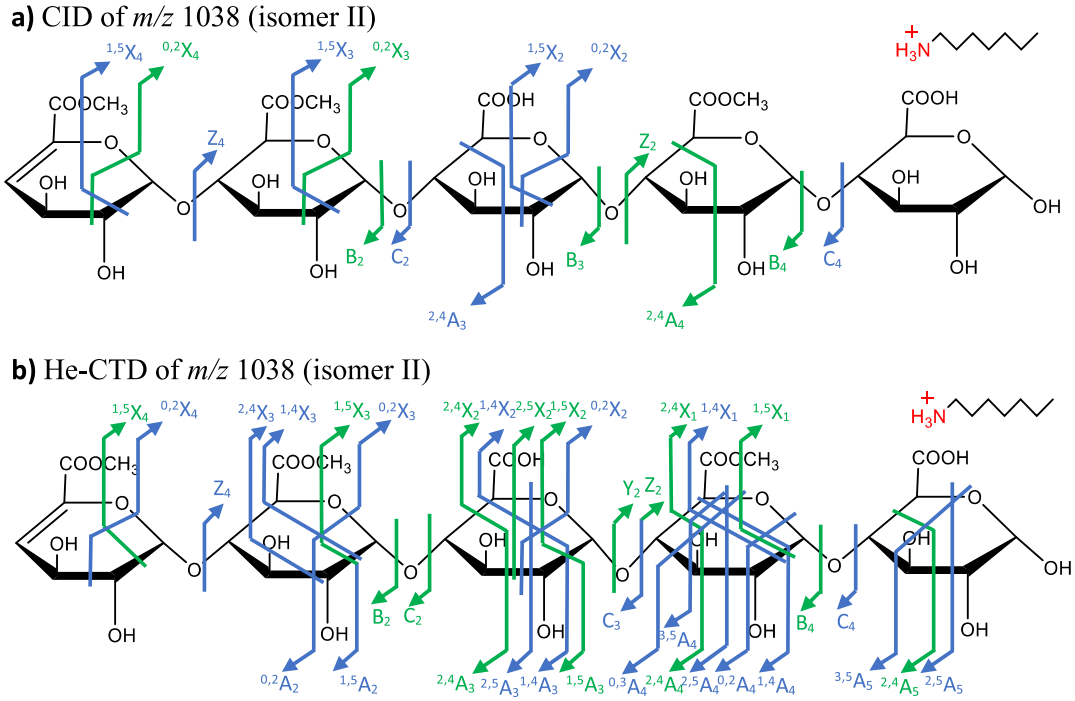

Figure 6. Fragmentation patterns for oligogalacturonan DP5DM3 (isomer II) eluting at 10.9 min. Blue annotations are ambiguous because of alternative isobaric annotations. Green annotations are unambiguous.

structures and their observed fragments are summarized in Figures 5, 6 and S2, respectively. The corresponding spectra for DP5DM3 are shown in Figures S3−S5. CID did not provide sufficient structural information to identify the methyl-esterificaation positions or linkage patterns between the Gal A units of the isomeric structures. However, CID produced glycosidic products that can be used to differentiate each isomer. For isomer I and II, the unambiguous B_4 fragment indicates the inclusion of three methyl groups toward the nonreducing end, which help to identify the presence of nonmethylated Gal A unit at the reducing end. This knowledge helps to distinguish between isomers I and II from isomer III, the latter of which has a methylated Gal A unit at the reducing end, as indicated by the ambiguous Z_2 fragment. The Z_2 fragment for isomer I is ambiguous because it is only observed in combination with small neutral losses, and the fragment overlaps with neutral losses from B_2 or C_2 fragments. The unambiguous B_2 fragment of isomer II indicates that this isomer contains two methyl groups on the nonreducing end, which help to distinguish isomer II from isomers I and III.

In cases where the ambiguity in peak assignments is due to fragments from different ends of the oligosaccharide, such ambiguity could theoretically be resolved by heavy oxygen labeling (^{18}O).[1,8] However, in this work, these spectra are shown only to compare and contrast the CID results with the He-CTD results, the latter of which provide less ambiguous fragments, even in the absence of ^{18}O labeling.

Using CID, the unambiguous Z_2 fragment of isomer III indicates the presence of two methyl groups on the reducing end sugars, which helps to distinguish itself from isomers I and II. CID produced several cross-ring cleavages including ions with one or more of the possible structures of $^{1,5}X_n$, $^{0,2}X_n$, or $^{2,4}A_n$. Similar to the other structures discussed above, these possible cross-ring fragments are observed in combination with multiple neutral losses, including the structurally important methyl groups. The neutral losses of methanol add uncertainty in localizing the methyl ester sites in each isomer. In contrast to CID, He-CTD provides more structurally informative fragments, such as cross-ring cleavages with fewer neutral losses. He-CTD provided abundant $^{1,5}X_n$ and $^{2,4}X_n$ fragments without any methyl group losses, which is highly advantageous in localizing methyl groups not just on a particular Gal A unit, but in several cases within each one.

For all three isomers, the presence of a methylated Gal A unit at the nonreducing end can be recognized by the unambiguous $^{1,5}X_4$ fragment because for all three isomers, the $^{1,5}X_4$ fragment includes only two of the three methyl groups. For isomer I, the locations of the second and third methylated Gal A units can be identified with the aid of the unambiguous $^{1,5}X_2-Y_3$ pair and unambiguous $^{1,5}X_1-Y_2$ fragment pairs. The possible $^{0,3}A_n$ or $^{1,4}X_n$ fragments, in combination with abundant $^{1,5}X_n$ ions, can be used to identify the methylated site at the 6-*O* position. The characteristic $^{2,4}A_5$ fragment is seen in all three isomers and is useful in obtaining information regarding methyl-esterification on the reducing terminus.

These results demonstrate the ability to collect real-time UHPLC-CTD-MS spectra, which provide more information about the structure of isomeric oligosaccharides in a mixture compared to a conventional UHPLC-CID-MS. Whereas previous reports of He-CTD have benefitted from direct infusion experiments, which enabled more than a minute of signal averaging for each analyte, the results of this work indicate that the signal to noise ratios obtained in real-time separations are still adequate for resolving questions about the structural identity of structural isomers. The results of He-CTD for oligogalacturonans show the same distinctive characteristics as reported in XUV-DPI experiments, with the production of cross-ring fragments such as $^{1,5}X_n$, $^{0,2}X_n$, and $^{2,4}A_n$ by both techniques.[8] The fragments generated by He-CTD show similarities to the cross-ring fragmentation patterns

https://dx.doi.org/10.1021/acs.analchem.0c04142
Anal. Chem. 2021, 93, 2838−2847

observed with acidic oligosaccharides such as GAGs analyzed with EDD.[37] The methyl groups are more stable than the sulfate modifications on glycan structures, and previous studies have shown that He-CTD preserves both modifications in the majority of generated fragments.[37,8] In the current application, the observed isomers inform the reader both about the nature of the digestive enzyme that was used to generate the mixture and about the frequency of certain methyl-esterification patterns within this particular sample of a highly methylated pectin. Such capabilities are important for understanding plant biochemistry and the structure/function relationship of different plant products that are based on these types of polysaccharides.

CONCLUSIONS

This first coupling of CTD with UHPLC provides compelling evidence that the CTD spectra are of sufficient quality and signal-to-noise ratio to provide more confident structural characterization of the complex oligogalacturonan mixtures than can UHPLC-CID-MS on the same instrument. The timescale of CTD—that is, 50 ms of ion activation followed by a 200 ms delay to reduce background interference—enables more than five tandem mass spectra to be acquired across each chromatographic peak, which is sufficient for modest spectral averaging. The benefits of interpreting He-CTD spectra are due to a combination of an increase in the abundance of cross-ring cleavages and a reduction in the abundance of small neutral losses that accompany each fragment. Therefore, in contrast to CID, more of the fragments in He-CTD are unambiguous, even without the potential benefit of heavy oxygen labeling on the reducing terminus. Unlike CID, He-CTD often produces multiple X and A ions within each Gal A unit, which also helps to confirm the 6-*O* -methyl-esterification position and the linkage positions between Gal A units. Future work intends to assess whether or not the beneficial cross-ring cleavages obtained through UHPLC-CTD-MS will be as effective in oligomers that contain different linkage positions, branching positions, or functional groups to extend the range of applications to glycosaminoglycans, among others.

ASSOCIATED CONTENT

Supporting Information

The Supporting Information is available free of charge at https://pubs.acs.org/doi/10.1021/acs.analchem.0c04142.

Experimental details, the total ion chromatogram of the oligogalacturonan mixture shown in Figure 1, a fragment ion map of DP5DM3 isomer III, and CID and He-CTD spectra of the three isomers of DP5DM3 (PDF)

AUTHOR INFORMATION

Corresponding Author

Glen P. Jackson − *C. Eugene Bennett Department of Chemistry and Department of Forensic and Investigative Science, West Virginia University, Morgantown, West Virginia 26506-6121, United States;* orcid.org/0000-0003-0803-6254; Phone: +1(304) 293-9236; Email: glen.jackson@mail.wvu.edu

Authors

Praneeth M. Mendis − *C. Eugene Bennett Department of Chemistry, West Virginia University, Morgantown, West Virginia 26506-6121, United States*

Zachary J. Sasiene − *C. Eugene Bennett Department of Chemistry, West Virginia University, Morgantown, West Virginia 26506-6121, United States*

David Ropartz − *INRAE, UR BIA, Nantes F-44316, France; INRAE, BIBS Facility, Nantes F-44316, France;* orcid.org/0000-0003-4767-6940

Hélène Rogniaux − *INRAE, UR BIA, Nantes F-44316, France; INRAE, BIBS Facility, Nantes F-44316, France;* orcid.org/0000-0001-6083-2034

Complete contact information is available at: https://pubs.acs.org/10.1021/acs.analchem.0c04142

Notes

The authors declare no competing financial interest.

ACKNOWLEDGMENTS

This work was supported by the National Science Foundation (NSF) (CHE-1710376) and the National Institute of Health (NIH) (1R01GM114494-01). The opinions, findings and conclusions or recommendations expressed in this publication are those of the author(s) and do not necessarily reflect the views of NSF or NIH.

REFERENCES

(1) Ropartz, D.; Lemoine, J.; Giuliani, A.; Bittebière, Y.; Enjalbert, Q.; Antoine, R.; Dugourd, P.; Ralet, M.-C.; Rogniaux, H. *Anal. Chim. Acta* **2014**, *807*, 84−95.

(2) Daas, P. J. H.; Arisz, P. W.; Schols, H. A.; De Ruiter, G. A.; Voragen, A. G. J. *Anal. Biochem.* **1998**, *257*, 195−202.

(3) Mutenda, K. E.; Körner, R.; Christensen, T. M. I. E.; Mikkelsen, J.; Roepstorff, P. *Carbohydr. Res.* **2002**, *337*, 1217−1227.

(4) Ralet, M.-C.; Williams, M. A. K.; Tanhatan-Nasseri, A.; Ropartz, D.; Quéméner, B.; Bonnin, E. *Biomacromolecules* **2012**, *13*, 1615−1624.

(5) Bonnin, E.; Garnier, C.; Ralet, M.-C. *Appl. Microbiol. Biotechnol.* **2014**, *98*, 519−532.

(6) Körner, R.; Limberg, G.; Christensen, T. M. I. E.; Mikkelsen, J. D.; Roepstorff, P. *Anal. Chem.* **1999**, *71*, 1421−1427.

(7) Han, L.; Costello, C. E. *Biochem* **2013**, *78*, 710−720.

(8) Ropartz, D.; Li, P.; Fanuel, M.; Giuliani, A.; Rogniaux, H.; Jackson, G. P. *J. Am. Soc. Mass Spectrom.* **2016**, *27*, 1614−1619.

(9) Johnson, A. R.; Carlson, E. E. *Anal. Chem.* **2015**, *87*, 10668−10678.

(10) Kailemia, M. J.; Ruhaak, L. R.; Lebrilla, C. B.; Amster, I. J. *Anal. Chem.* **2014**, *86*, 196−212.

(11) Syka, J. E. P.; Coon, J. J.; Schroeder, M. J.; Shabanowitz, J.; Hunt, D. F. *Proc. Natl. Acad. Sci. U.S.A.* **2004**, *101*, 9528−9533.

(12) Adamson, J. T.; Håkansson, K. *Anal. Chem.* **2007**, *79*, 2901−2910.

(13) Han, L.; Costello, C. E. *J. Am. Soc. Mass Spectrom.* **2011**, *22*, 997−1013.

(14) Wolff, J. J.; Leach, F. E., III; Laremore, T. N.; Kaplan, D. A.; Easterling, M. L.; Linhardt, R. J.; Amster, I. J. *Anal. Chem.* **2010**, *82*, 3460−3466.

(15) Wolff, J. J.; Chi, L.; Linhardt, R. J.; Amster, I. J. *Anal. Chem.* **2007**, *79*, 2015−2022.

(16) Wolff, J. J.; Amster, I. J.; Chi, L.; Linhardt, R. J. *J. Am. Soc. Mass Spectrom.* **2007**, *18*, 234−244.

(17) Yu, X.; Jiang, Y.; Chen, Y.; Huang, Y.; Costello, C. E.; Lin, C. *Anal. Chem.* **2013**, *85*, 10017−10021.

(18) Wolff, J.; Laremore, T.; Aslam, H.; Linhardt, R.; Amster, I. J. *J. Am. Soc. Mass Spectrom.* **2008**, *19*, 1449−1458.

(19) Huang, Y.; Yu, X.; Mao, Y.; Costello, C. E.; Zaia, J.; Lin, C. *Anal. Chem.* **2013**, *85*, 11979−11986.

(20) Tang, Y.; Wei, J.; Costello, C. E.; Lin, C. *J. Am. Soc. Mass Spectrom.* **2018**, *29*, 1295−1307.

(21) Wei, J.; Tang, Y.; Ridgeway, M. E.; Park, M. A.; Costello, C. E.; Lin, C. *Anal. Chem.* **2020**, *92*, 13211−13220.
(22) Fort, K. L.; Cramer, C. N.; Voinov, V. G.; Vasil'ev, Y. V.; Lopez, N. I.; Beckman, J. S.; Heck, A. J. R. *J. Proteome Res.* **2018**, *17*, 926−933.
(23) Devakumar, A.; Thompson, M. S.; Reilly, J. P. *Rapid Commun. Mass Spectrom.* **2005**, *19*, 2313−2320.
(24) Ropartz, D.; Giuliani, A.; Hervé, C.; Geairon, A.; Jam, M.; Czjzek, M.; Rogniaux, H. *Anal. Chem.* **2015**, *87*, 1042−1049.
(25) Devakumar, A.; Mechref, Y.; Kang, P.; Novotny, M. V.; Reilly, J. P. *Rapid Commun. Mass Spectrom.* **2007**, *21*, 1452−1460.
(26) Devakumar, A.; Mechref, Y.; Kang, P.; Novotny, M.; Reilly, J. *J. Am. Soc. Mass Spectrom.* **2008**, *19*, 1027−1040.
(27) Reilly, J. P. *Mass Spectrom. Rev.* **2009**, *28*, 425−447.
(28) Murtada, R.; Fabijanczuk, K.; Gaspar, K.; Dong, X.; Alzarieni, K. Z.; Calix, K.; Manriquez, E.; Bakestani, R. M.; Kenttämaa, H. I.; Gao, J. *Anal. Chem.* **2020**, *92*, 13794−13802.
(29) Desai, N.; Thomas, D. A.; Lee, J.; Gao, J.; Beauchamp, J. L. *Chem. Sci.* **2016**, *7*, 5390−5397.
(30) Ropartz, D.; Li, P.; Jackson, G. P.; Rogniaux, H. *Anal. Chem.* **2017**, *89*, 3824−3828.
(31) Li, P.; Kreft, I.; Jackson, G. P. *J. Am. Soc. Mass Spectrom.* **2018**, *29*, 284−296.
(32) Li, P.; Jackson, G. P. *J. Mass Spectrom.* **2017**, *52*, 271−282.
(33) Bari, S.; Hoekstra, R.; Schlathölter, T. *Phys. Chem. Chem. Phys.* **2010**, *12*, 3376−3383.
(34) Bari, S.; Hoekstra, R.; Schlathölter, T. *Int. J. Mass Spectrom.* **2011**, *299*, 64−70.
(35) Chingin, K.; Makarov, A.; Denisov, E.; Rebrov, O.; Zubarev, R. A. *Anal. Chem.* **2014**, *86*, 372−379.
(36) Hoffmann, W. D.; Jackson, G. P. *J. Am. Soc. Mass Spectrom.* **2014**, *25*, 1939−1943.
(37) Pepi, L. E.; Sasiene, Z. J.; Mendis, P. M.; Jackson, G. P.; Amster, I. J. *J. Am. Soc. Mass Spectrom.* **2020**, *31*, 2143−2153.
(38) Huang, Y.; Zhou, S.; Zhu, J.; Lubman, D. M.; Mechref, Y. *Electrophoresis* **2017**, *38*, 2160−2167.
(39) Melmer, M.; Stangler, T.; Premstaller, A.; Lindner, W. *J. Chromatogr. A* **2011**, *1218*, 118−123.
(40) Brustkern, A. M.; Buhse, L. F.; Nasr, M.; Al-Hakim, A.; Keire, D. A. *Anal. Chem.* **2010**, *82*, 9865−9870.
(41) Thurl, S.; Müller-Werner, B.; Sawatzki, G. *Anal. Biochem.* **1996**, *235*, 202−206.
(42) Wuhrer, M.; de Boer, A. R.; Deelder, A. M. *Mass Spectrom. Rev.* **2009**, *28*, 192−206.
(43) Zhang, Z.; Xie, J.; Liu, H.; Liu, J.; Linhardt, R. J. *Anal. Chem.* **2009**, *81*, 4349−4355.
(44) Bao, Y.; Chen, C.; Newburg, D. S. *Anal. Biochem.* **2013**, *433*, 28−35.
(45) Wei, J.; Tang, Y.; Bai, Y.; Zaia, J.; Costello, C. E.; Hong, P.; Lin, C. *Anal. Chem.* **2020**, *92*, 782−791.
(46) Ji, D.; Roman, M.; Zhou, J.; Hildreth, J. *J. AOAC Int.* **2007**, *90*, 659−669.
(47) Pabst, M.; Altmann, F. *Anal. Chem.* **2008**, *80*, 7534−7542.
(48) Antonopoulos, A.; Favetta, P.; Helbert, W.; Lafosse, M. *Carbohydr. Res.* **2004**, *339*, 1301−1309.
(49) Ropartz, D.; Giuliani, A.; Fanuel, M.; Hervé, C.; Czjzek, M.; Rogniaux, H. *Anal. Chim. Acta* **2016**, *933*, 1−9.
(50) Harvey, D. J.; Bateman, R. H.; Green, M. R. *J. Mass Spectrom.* **1997**, *32*, 167−187.
(51) Tang, Y.; Pu, Y.; Gao, J.; Hong, P.; Costello, C. E.; Lin, C. *Anal. Chem.* **2018**, *90*, 3793−3801.
(52) Buck-Wiese, H.; Fanuel, M.; Liebeke, M.; Le Mai Hoang, K.; Pardo-Vargas, A.; Seeberger, P. H.; Hehemann, J.-H.; Rogniaux, H.; Jackson, G. P.; Ropartz, D. *J. Am. Soc. Mass Spectrom.* **2020**, *31*, 1249−1259.

https://dx.doi.org/10.1021/acs.analchem.0c04142
Anal. Chem. 2021, 93, 2838−2847